Electronic Supplementary Material (ESI) for Physical Chemistry Chemical Physics.


# Ligand-induced action of the W286$^{6.48}$ rotamer toggle switch in $\beta_2$-adrenergic receptor

**Anita Plazinska, Wojciech Plazinski, Rafal Luchowski, Artur Wnorowski, Wojciech Grudzinski, Wieslaw I. Gruszecki**

## Supporting Information

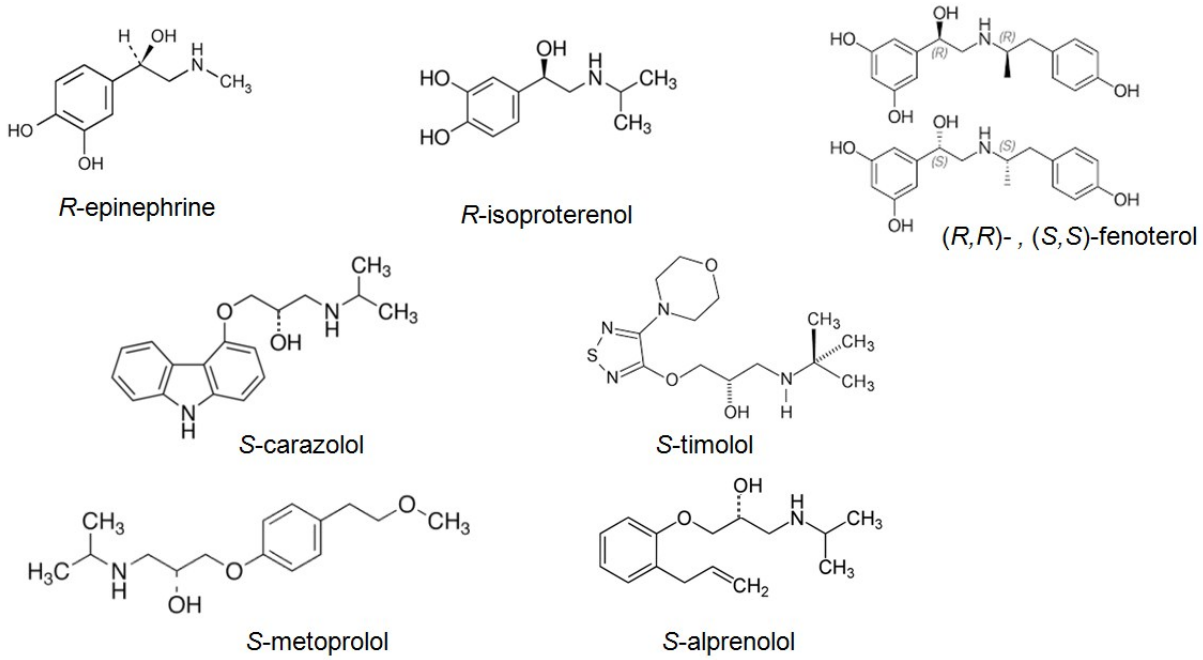


**Fig. S1.** The structures of compounds used in the computational part of the study. The experimental TRFS study concerned *R*-epinephrine.

**Tab. S1.** Molecular systems studied during MD simulations.

| System number | ligand | Conformation of the receptor | Point mutation | Simulation type[#] |
|---|---|---|---|---|
| **agonists** | | | | |
| 1 | (*R*)-epinephrine | Ac_β2-AR | None | LEUS, unbiased MD |
| 2 | (*R*)-epinephrine | Ac_β2-AR | F289A | - |
| 3 | (*R*)-epinephrine | Ac_β2-AR | F290A | - |
| 4 | (*R*)-epinephrine | Ac_β2-AR | Y209A | - |
| 5 | (*R*)-epinephrine | Ac_β2-AR | Y308A | - |
| 6 | (*R*)-epinephrine | In_β2-AR | None | - |
| 7 | (*R*)-isoproterenol | Ac_β2-AR | None | - |
| 8 | (*R*,*R*)-fenoterol | Ac_β2-AR | None | - |
| 9 | (*R*,*R*)-fenoterol | Ac_β2-AR | Y308A | - |
| 10 | (*R*,*R*)-fenoterol | In_β2-AR | None | - |
| 11 | (*S*,*S*)-fenoterol | Ac_β2-AR | None | - |
| **antagonists** | | | | |
| 12 | (*S*)-alprenolol | In_β2-AR | None | - |
| 13 | (*S*)-metoprolol | In_β2-AR | None | - |
| **inverse agonists** | | | | |
| 14 | (*S*)-carazolol | In_β2-AR | None | - |
| 15 | (*S*)-carazolol | Ac_β2-AR | None | - |
| 16 | (*S*)-timolol | In_β2-AR | None | - |
| ***apo*-forms** | | | | |
| 17 | - | In_β2-AR | None | LEUS, unbiased MD, MD with W286 constrained in OS, MD with W286 constrained in CS |
| 18 | - | Ac_β2-AR | None | unbiased MD, MD with W286 constrained in OS, MD with W286 constrained in CS |
| 19 | - | Ac_β2-AR | Y308A | - |

[#] Not including the equilibration stage and FEMs calculations (metadynamics) which were applied for all the systems.

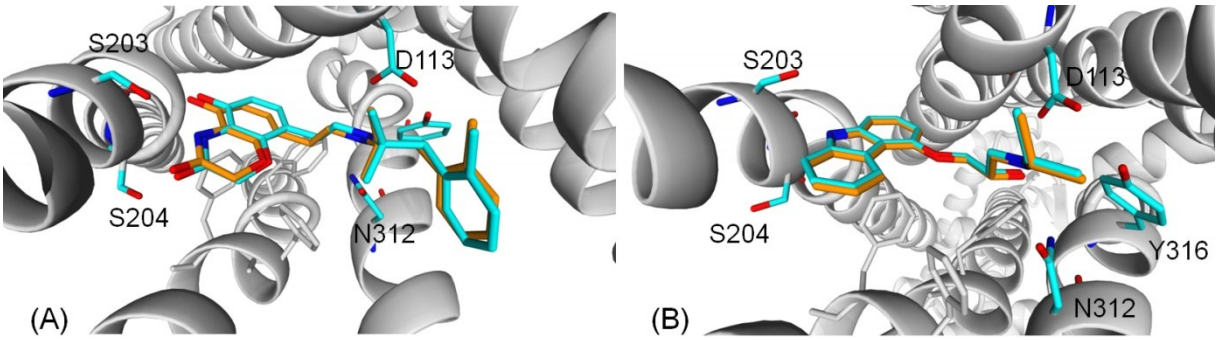


**Fig. S2.** The validation of the accepted docking algorithm by comparison of the structures obtained in the result of the docking procedure (coloured in orange) with those resolved on the basis of experimental (XRD) studies (coloured in element). The considered ligands were: BI-167107 (A, agonist) and *S*-carazolol (B, inverse agonist) and the root mean square deviation parameter calculated for position of all ligand atoms of equals to 0.27 Å and 0.11 Å, respectively.

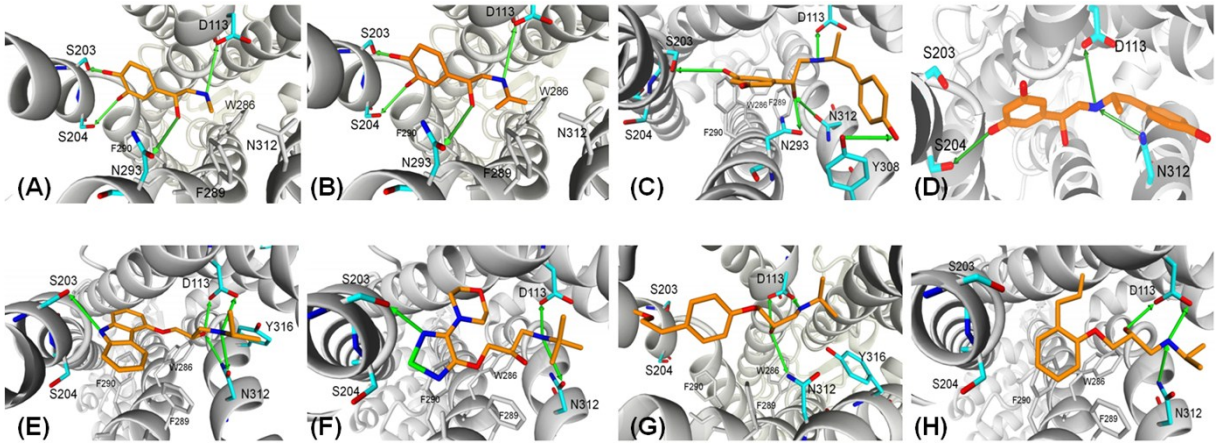


**Fig. S3.** The depiction of the most energetically favourable structures (i.e. characterized by the lowest MolDock Score [kJ/mol] values; see Tab. S2) of the ligand-receptor complexes. These structures were used as a starting points for MD simulations: (*R*)-epinephrine (A), (*R*)-isoproterenol (B); (*R*,*R*)-fenoterol (C), (*S*,*S*)-fenoterol (D) (*S*)-carazolol (E), (*S*)-timolol (F), (*S*)-metoprolol (G), (*S*)-alprenolol (H).

**Tab. S2.** The lowest MolDock Score values obtained for the $\beta_2$-AR-ligand complexes during docking procedure and corresponding to the structures shown in Fig. S3.

| **Ligand** | **MolDock Score [kJ/mol]** |
|---|---|
| *R*-epinephrine | -127.824 |
| *R*-isoproterenol | -129.109 |
| (*R,R*)-fenoterol | -133.699 |
| (*S,S*)-fenoterol | -134.607 |
| *S*-carazolol | -136.322 |
| *S*-timolol | -117.783 |
| *S*-metoprolol | -131.541 |
| *S*-alprenolol | -128.113 |

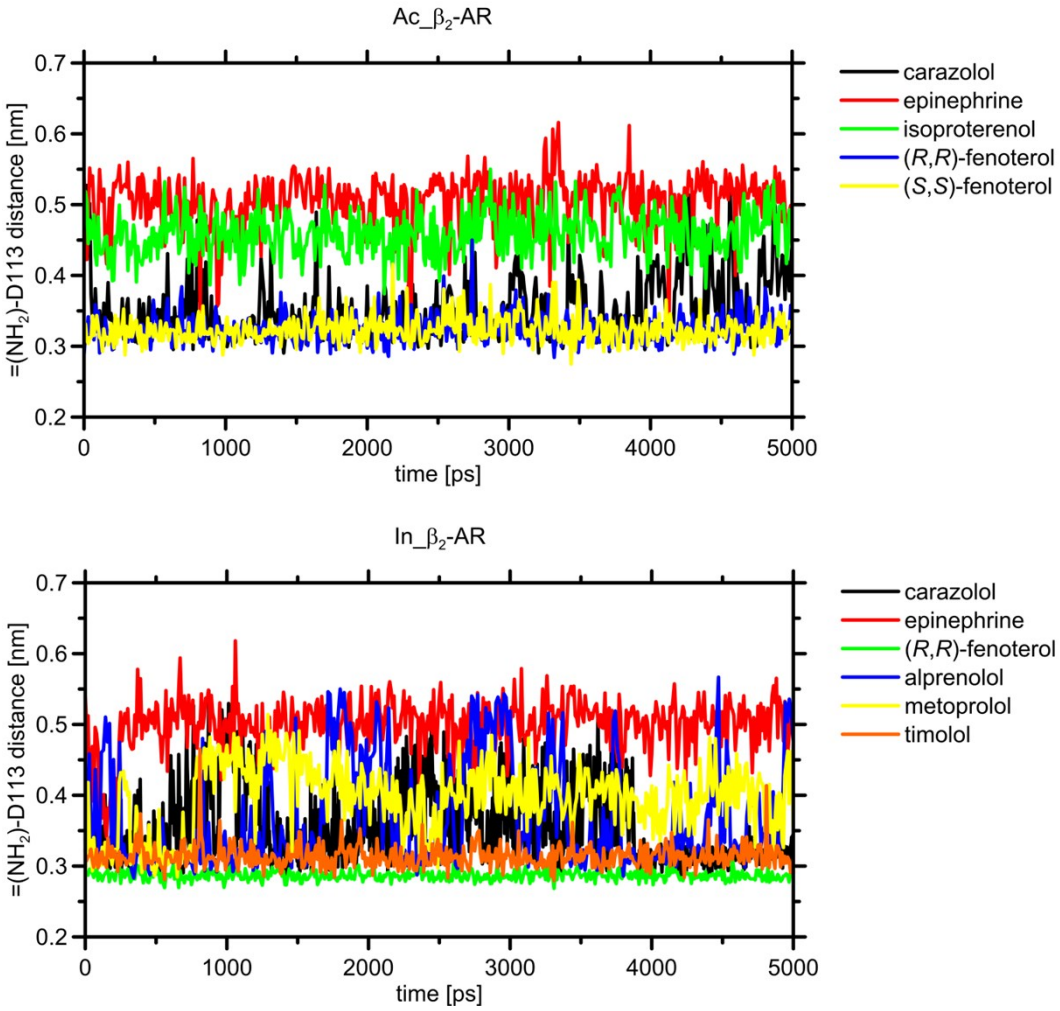


**Fig. S4.** The distance between the negatively charged D113 residue and the amine moiety of different ligand molecules. The distances were monitored during unbiased MD (5 ns-long equilibration stage under NPT conditions).

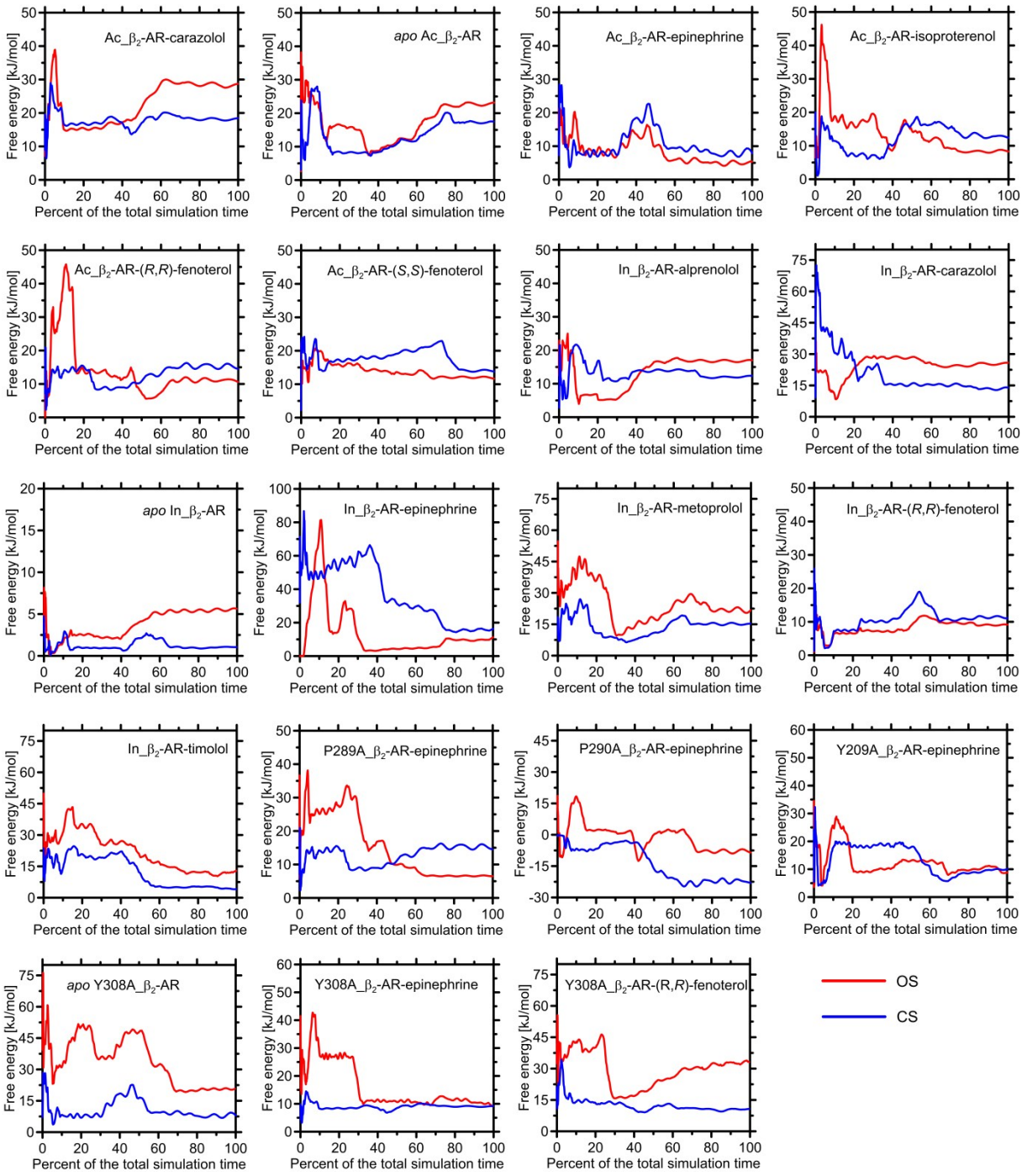


**Fig. S5.** The convergence of the relative free energies of the OS and CS conformational states of the W286 residue (calculated with respect to the energy of the GS state). The calculations rely on the metadynamics calculations of length varying between 75 and 120 ns. The averaged final energies are shown in Figs. 4 and 5 (main manuscript).

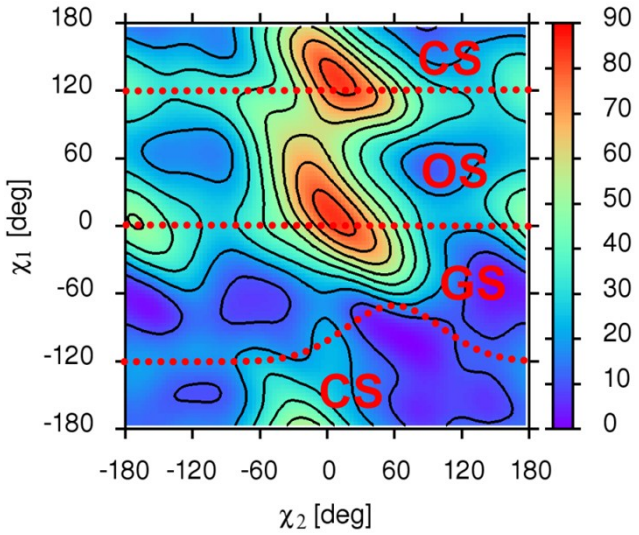


**Fig. S6.** The assignment scheme used to quantitatively describe the free energy differences between the CS, GS and OS conformational states of W286. The illustrative FEM corresponds to the *apo*-In_$\beta_2$-AR system. The division of the phase space was made on the basis of the insight into MD trajectories and orientation of the W286 sidechain with respect to the inner receptor channel. The dotted lines represent either a constant values ($\chi_1 = \pm 120$ deg and $\chi_1 = 0$) or a more complex function ($\chi_1 = -120 + 50 \exp(-((-\chi_2 - 60)/60)^2)$) reflecting the existence of minimum 5. The assignment scheme is common for all calculated FEMs.

**Tab. S3.** Radial distribution functions calculated for the distance between the tryptophan sidechain and water molecules and integrated in the range 0-1.2 nm. Both standard (30 ns-long) molecular dynamics simulations (MD) and the LEUS protocol based on the 2D free energy maps (LEUS-MD) were employed (see details in the main manuscript). The environment of the given tryptophan sidechain was classified as exhibiting hydrophobic, hydrophilic or intermediate character based on arbitrary accepted limiting values equal to 50 and 100. Note that the LEUS procedure is necessary to obtain the correct distribution of water molecules around W286 which accounts for all the contribution of all the relevant conformers.

| | Ac_β2-AR-epinephrine | | In_β2-AR | |
|---|---|---|---|---|
| W residues | Integral of RDFs (0-1.2 nm) | | Integral of RDFs (0-1.2 nm) | |
| | MD | LEUS-MD | MD | LEUS-MD |
| **W286** | **74** | **109** | **86** | **76** |
| W313 | 62 | 66 | 39 | 36 |
| W173 | 55 | 54 | 181 | 180 |
| W158 | 20 | 20 | 19 | 20 |
| W109 | 112 | 111 | 89 | 83 |
| W105 | 75 | 75 | 81 | 80 |
| W99 | 153 | 154 | 163 | 164 |
| W32 | 260 | 261 | 145 | 147 |
| Classification of the environment of the tryptophan residues | | | | |
| Hydrophobic (< 50) | W: 158 | W: 158 | W: 158, 313 | W: 158, 313 |
| Intermediate (50-100) | W:105, 173, **286**, 313 | W:105, 173, 313 | W: 105, 109, **286** | W: 105, 109, **286** |
| Hydrophilic (> 100) | W: 32, 99, 109 | W: 32, 99, 109, **286** | W: 32, 99, 173 | W:32, 99, 173 |

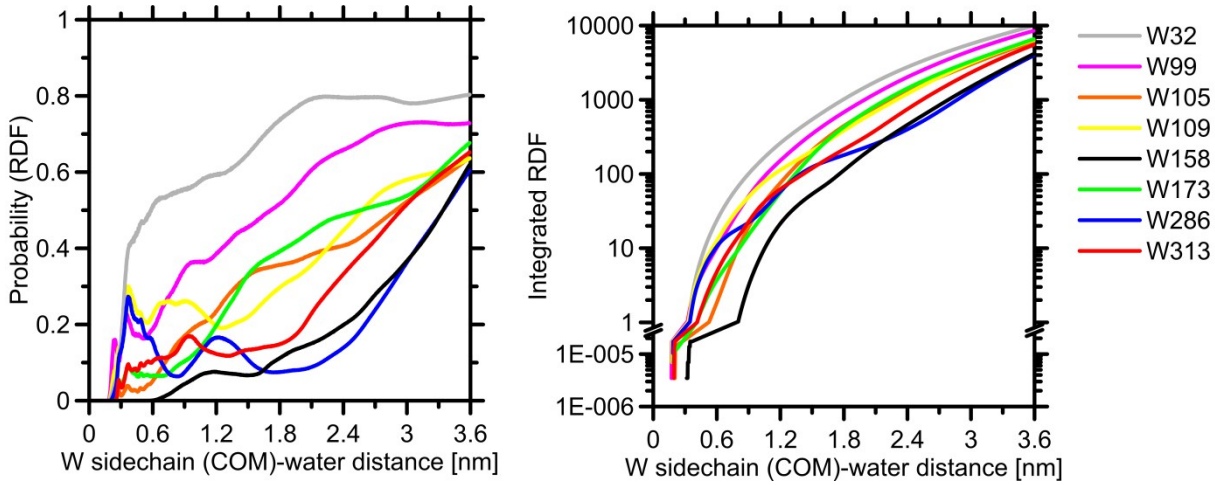


**Fig. S7.** (*left*) RDFs calculated for all the possible tryptophan-water pairs that exist in the system containing unliganded In_β2-AR. (*right*) The integrated RDFs providing a quantitative description of the solvation state of the given tryptophan residue. The results rely on the 30 ns-long unbiased MD simulations.

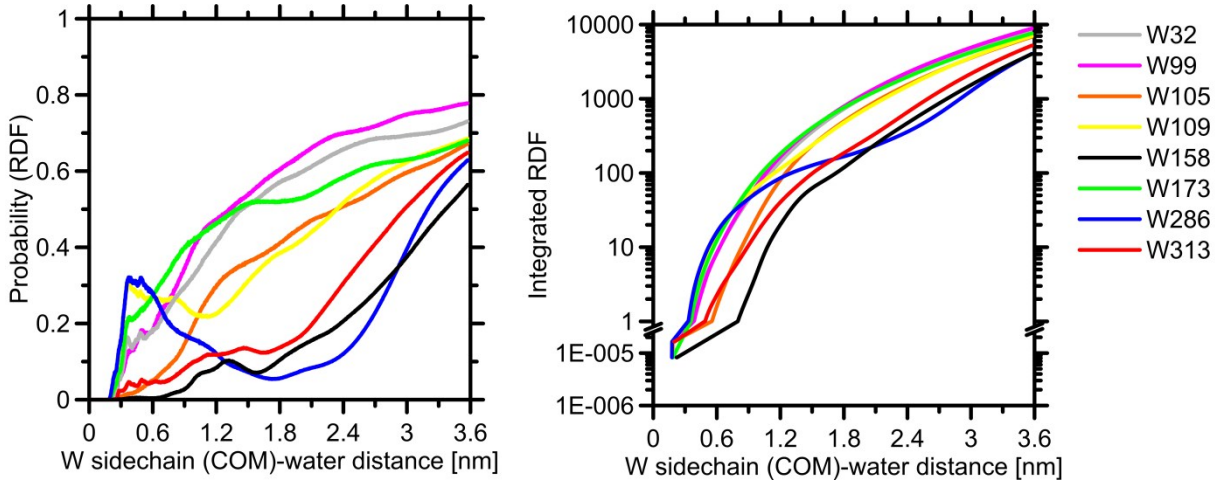


**Fig. S8.** (*left*) RDFs calculated for all the possible tryptophan-water pairs that exist in the system containing the Ac_β2-AR-epinephrine complex. (*right*) The integrated RDFs providing a quantitative description of the solvation state of the given tryptophan residue. The results rely on the 30 ns-long unbiased MD simulations.

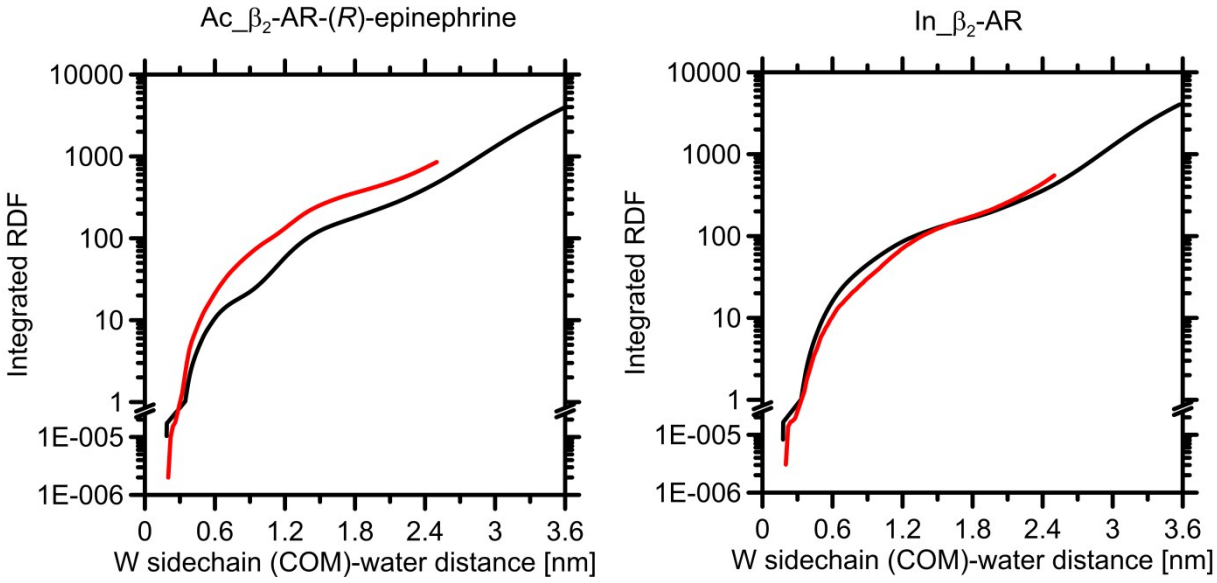


**Fig. S9**. The integrated RDFs providing a quantitative description of the solvation state of the given residue for the two molecular systems which were studied experimentally (i.e. the Ac_β2-AR-epinephrine complex and unliganded In_β2-AR). RDFs were calculated for the W286-water distance on the basis on either unbiased MD simulations lasting 30 ns (black lines) or on LEUS (biased) MD simulations (red lines), subsequently reweighted to obtain physically meaningful results. RDFs corresponding to the unbiased MD simulations are shown in Figs. S7 and S8.

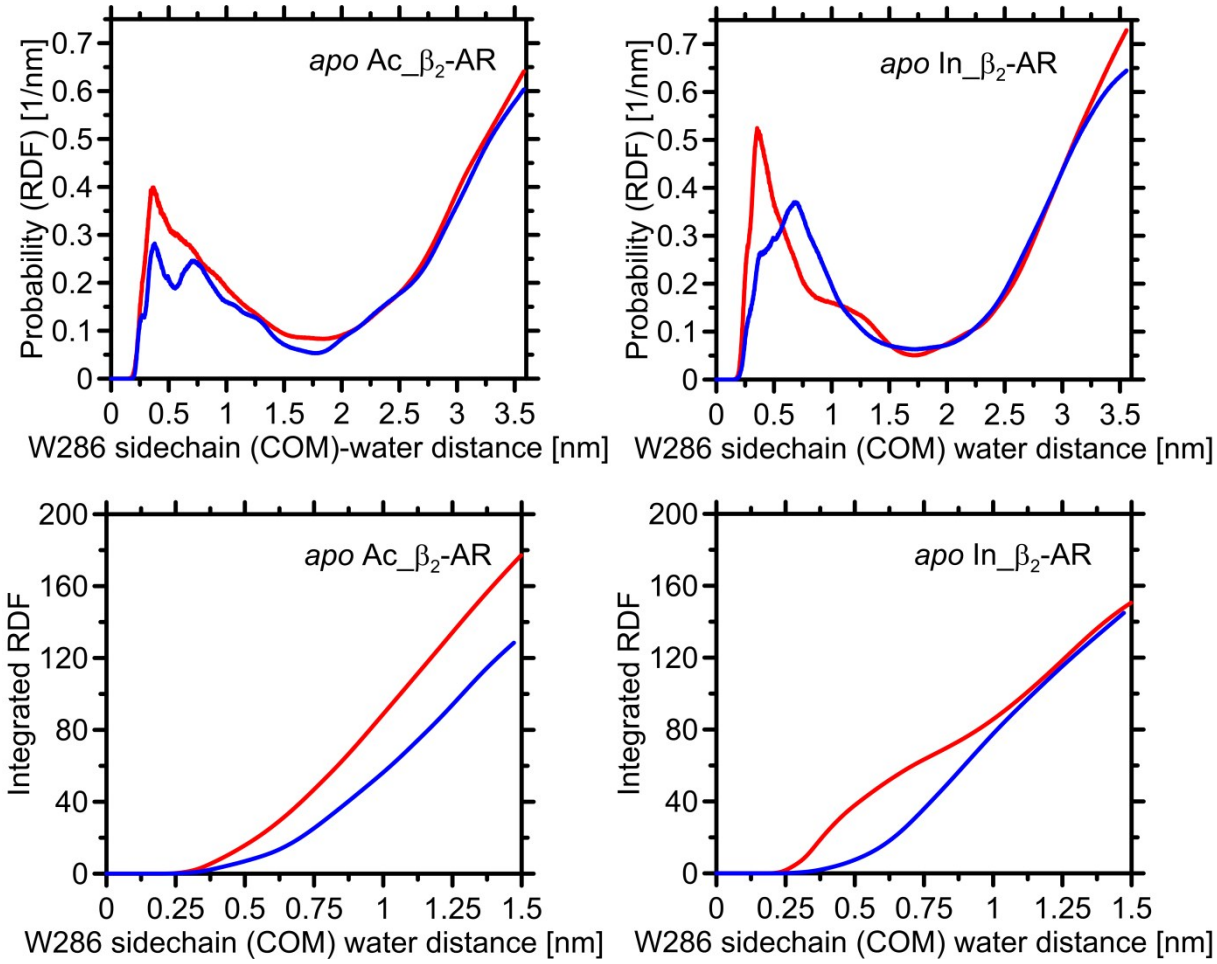


**Fig. S10.** The results of constrained MD simulations with the orientation of the W286 sidechain forced to either OS (red lines) or CS (blue lines) conformational states. Simulations concerned both In_β2-AR and Ac_β2-AR unliganded conformers. In the case of In_β2-AR the differences between RDF cancel out when considering the solvation degree at distance of 1.2 nm. On the contrary, the same differences remain for Ac_β2-AR, when considering the distances shorter than 1.5 nm. As the result the OS rotamers are associated with the larger solvation of W286 when considering the Ac_β2-AR conformer.

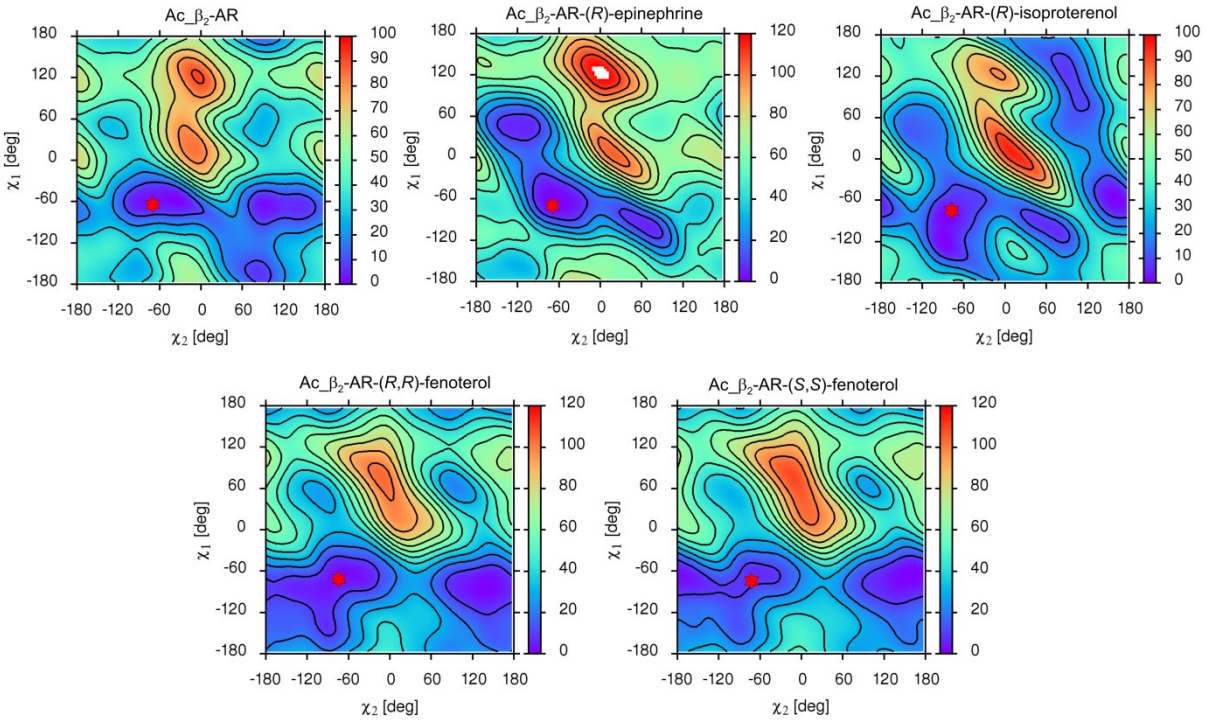


**Fig. S11.** FEMs describing the orientation of the W286$^{6.48}$ sidechain in the 'active' conformer of $\beta_2$-AR (either unliganded or bound to agonist ligand). Calculations relied on the metadynamics simulations in the 2D space defined by the two dihedral angles: $\chi_1$ vs. $\chi_2$ (see Fig. 2 for their definitions). The energy scale is in [kJ/mol]. The pink stars show the approximate location of the conformations extracted from the available crystal structures.

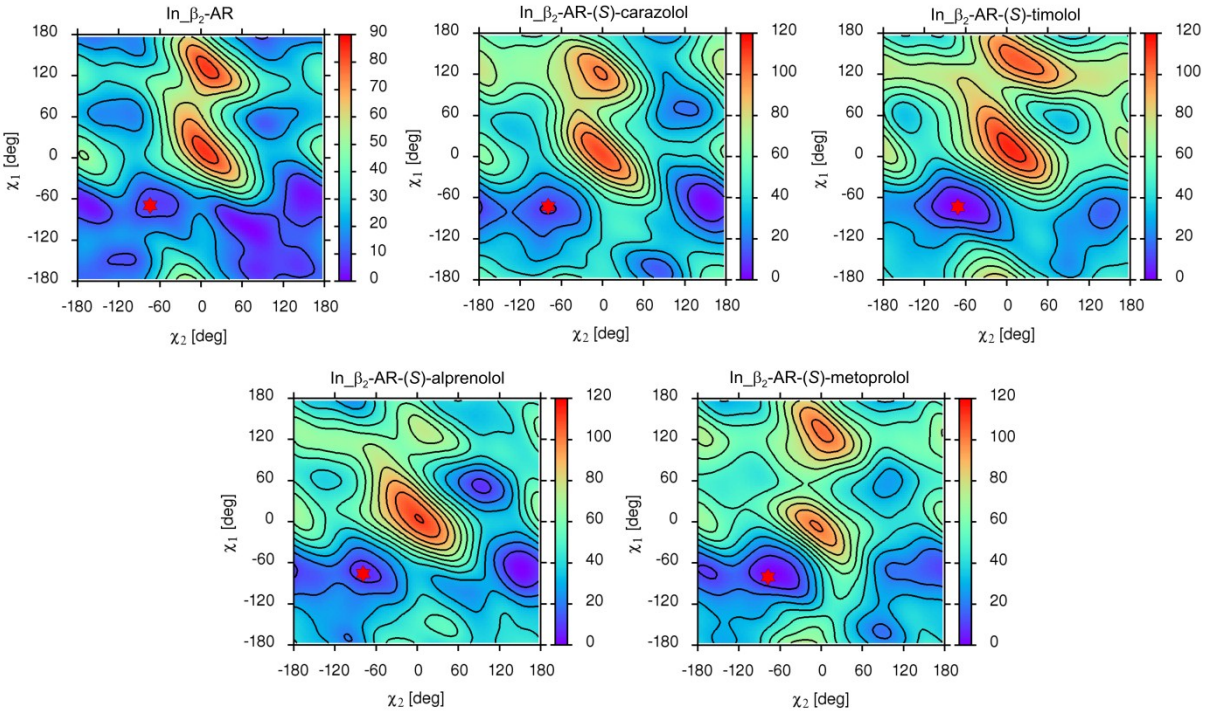


**Fig. S12.** FEMs describing the orientation of the W286$^{6.48}$ sidechain in the 'inactive' conformer of $\beta_2$-AR (either unliganded or bound to antagonist/inverse agonist ligand). The rest of details as in Fig. S11.

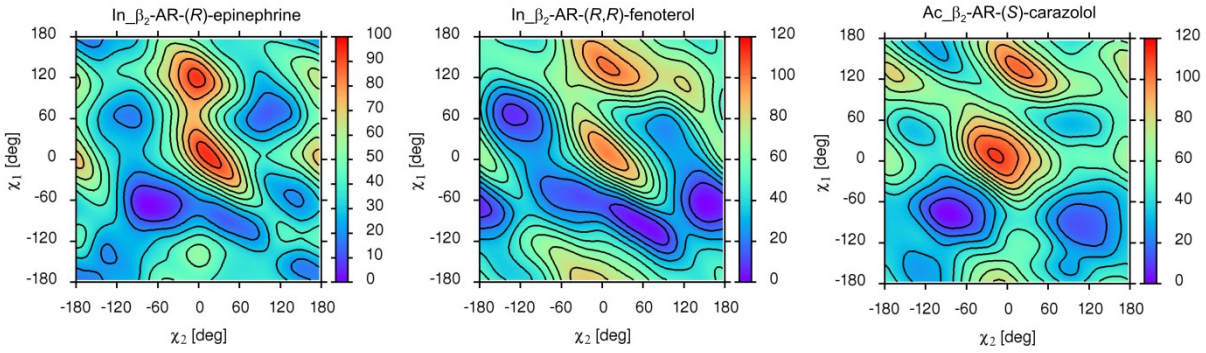


**Fig. S13.** FEMs describing the orientation of the W286 sidechain in the ligand-$\beta_2$-AR complexes when the ligand pharmacological character is not compatible with the receptor conformation. The rest of details as in Fig. S11.

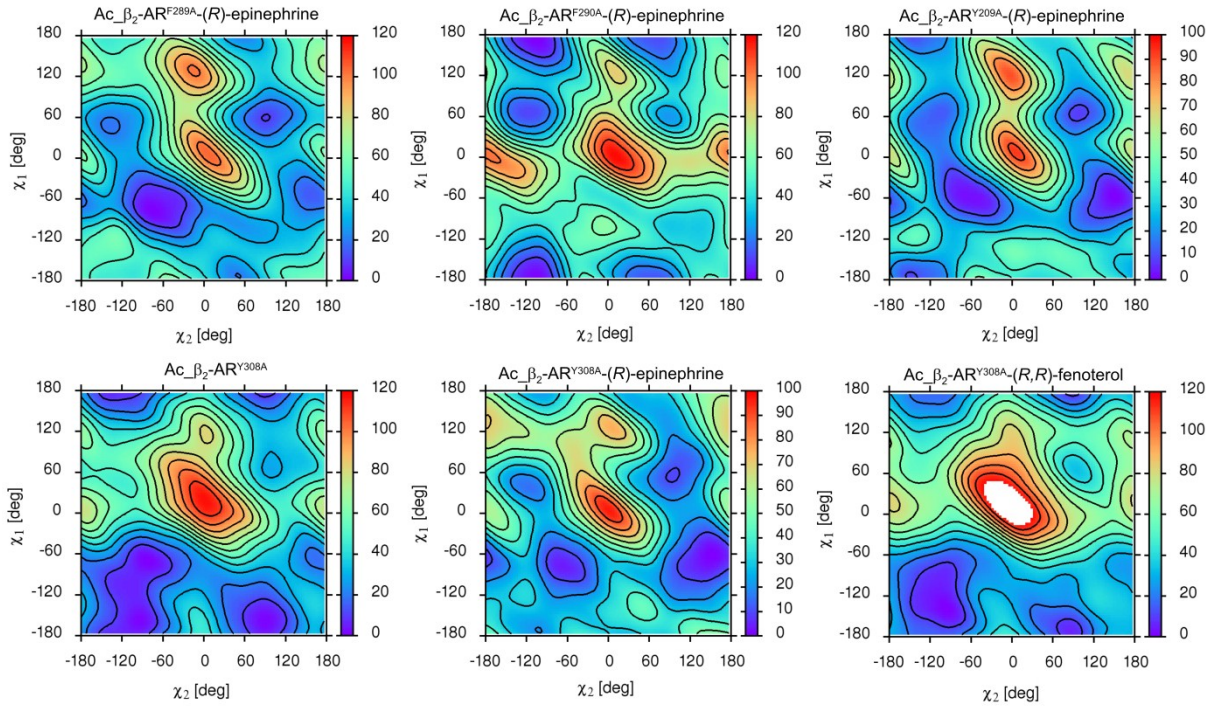


**Fig. S14.** FEMs describing the orientation of the W286$^{6.48}$ sidechain in the 'active' conformer of $\beta_2$-AR (either unliganded or bound to agonist ligand) containing point mutation. The rest of details as in Fig. S11.